A Tube Model of Rubber Elasticity

S. Kutter and E.M. Terentjev*
Cavendish Laboratory, University of Cambridge
Madingley Road, Cambridge CB3 0HE, U.K.

June 25, 2001

Abstract

Polymer entanglements lead to complicated topological constraints and interactions between neighbouring chains in a dense solution or melt. Entanglements can be treated in a mean field approach, within the famous reptation model, since they effectively confine each individual chain in a tube-like geometry. In polymer networks, due to crosslinks preventing the reptation constraint release, entanglements acquire a different topological meaning and have a much stronger effect on the resulting mechanical response. We apply the classical ideas of reptation dynamics to calculate the effective rubber-elastic free energy of an entangled rubbery network. We then compare the results with other theoretical approaches and establish a particularly close mapping with the hoop-model, with equally good description of experimental data. The present consistent reptation theory allows further development of dynamic theory of stress relaxation.

PACS numbers:
61.41.+e Polymers, elastomers, and plastics
62.20.Dc Elasticity, elastic constants

*Electronic mail: *emt1000@cam.ac.uk*

1 Introduction

Rubbery polymer networks are highly complex disordered systems. The simplest theoretical models consider them as being made of "phantom chains", where each polymer is modelled by a three-dimensional random walk in space. To form a corresponding phantom network, the chains are crosslinked to each other at their end points, but do not interact otherwise, in particular, they are able to fluctuate freely between crosslinks. This has the unphysical consequence that the strands can pass through each other. If one tries to avoid this assumption, the theory is confronted with the intractable complexity of entanglements and their topological constraints. The mean field treatment of entangled polymer systems is a now classical reptation theory (de Gennes 1979; Doi & Edwards 1986), which had a spectacular success in describing a large variety of different physical effects in melts and semi-dilute solutions. However, the parallel description of crosslinked rubbery networks has been much less successful. First of all, one has to appreciate a significant difference in the entanglement topology: in a polymer melt the confining chain has to be long enough to form a topological knot around a chosen polymer; even then the constraint is only dynamical and can be released by a reptation diffusion along the chain path. In a crosslinked network, any loop around a chosen strand becomes an entanglement, which could be mobile but cannot be released altogether. A number of other complexities arise from possible nematic interactions between rigid chain segments (Abramchuk *et al.* 1989; Bladon & Warner 1993) and from the coupling between imposed deformations and chain anisotropy known as the stress-optical effects (Jarry & Monnerie 1979; Deloche & Samulski 1981, Doi *et al.* 1989).

An early model of elastic response of entangled rubbers was developed by Edwards (1977): in tradition with the melt theory, it assumed that the presence of neighbouring strands in a dense network effectively confines a particular polymer strand to a tube, whose axis defines the primitive path, see Fig. 1. Within this tube, the polymer is free to explore all possible configurations, performing random excursions, parallel and perpendicular to the axis of the tube. One can show that on deformation the length of the primitive path increases. Since the arc length of the polymer is constant, the amount of chain available for perpendicular excursions is reduced, leading to a reduction in entropy and hence to an increase in free energy. However, the particular calculation in Edwards (1977) has a number of shortcomings; perhaps the main limitation is that one only looks at the entropy reduction associated with the overall change of primitive path contour length on deformation, ignoring the essential mechanisms of local reptation and segment re-distribution between different tube segments.

Gaylord and Douglas (GD) (1990) developed a simple "localisation model" for rubbers, based on scaling arguments. Each strand segment is thought to be placed in a hard tube of a square cross-section. Assuming that the deformation affinely changes the dimensions of the tube, one can calculate the change in free energy of a network of chains, each confined in such a tube. Ball, Doi, Edwards and Warner (BDEW) (1981) chose a completely different approach by introducing the "slip-link model": the effect of entanglements is not considered to be a permanent one, changing the environment of a single polymer strand as in the two models presented above, but rather leading to a local mobile confinement site, a link between two interwound strands, which is able to "slip" up and down along both strands. In a further development of this idea, Higgs and Ball (HB) (1989) adopted a similar approach, which is however mathematically much simpler: the entanglements localise certain short segments of a particular strand to a small volume. One can model this effect by describing a network strand as a free Gaussian random walk, which is, however, forced to pass through a certain number of hoops, which are fixed in space. We shall find that the results of HB are very close to ours, in spite of a number of significant differences in the physical model. This mapping gives confidence in the final expression for the rubber-elastic free energy and the role of network entanglements in it.

In addition to the mentioned above, one can find a variety of other theoretical models, some of which are discussed in the review article (Edwards & Vilgis 1988). For instance, the constrained junction fluctuation model (Flory & Erman 1982), which assumes that the entanglements primarily affect the fluctuation of the junction points. An overview of different models can be found for example in the reviews by Heinrich *et al.* (1995) and Han *et al.* (1999). All theoretical models, describing the macroscopic equilibrium elastic response of densely entangled rubbery networks, have a common purpose – to develop a physically consistent description depicting what one accepts as a correct coarse-grained molecular behaviour – but also accounting for a number of experimental results showing substantial deviations in stress-strain response from the ideal phantom-network result $\sigma = \mu(\lambda - 1/\lambda^2)$ (Higgs & Gaylord 1990). Up to now, no theory succeeded on both of these fronts.

In our current work, we develop a consistent implementation of the classical tube model to take into account the entanglement effects in crosslinked polymer networks within the same framework as in the polymer melt dynamics. We particularly focus on the entropy of internal reptation motion and resulting re-distribution of chain segments along the tube in a deformed state. The reptation tube model of entangled network strands provides a more accurate description in the sense that it keeps track of the allocation of chain segment excursions in the tubes. In this way, our model closes an im-

portant gap among the existing models with some unexpected consequences: the model, although based on existing ideas, analyses rubber elasticity in a new way. The calculations, however, reveal that our results are very similar to the ones of the HB model, which approaches rubber elasticity in a different way. After brief recollection of the principles of network theory on the example of the ideal phantom network in the following section, section 3 introduces the model and its properties in some detail, and outlines the derivation of the full expression for rubber-elastic free energy. Section 4 explores the properties of the full expression, examining different limiting cases, as well as its linear-response limit. We conclude by comparing the concepts and the results of this work with previous theories.

2 Classical phantom chain network

Before considering densely entangled rubber, we briefly review the well-known results of the phantom chain network theory, which provides the basics to most other theoretical models.

Assuming that a single polymer performs a free random walk in three dimensions, one finds that the end-to-end distance $\boldsymbol{R}_0$ obeys a Gaussian distribution in the long chain limit. This result goes back far in history: one can review its derivation and consequences in the classical text on this subject (Doi & Edwards 1986). The distribution of $\boldsymbol{R}_0$ is given by

$$P_0(\boldsymbol{R}_0) = \left(\frac{3}{2\pi N b^2}\right)^{3/2} \exp\left(-\frac{3}{2Nb^2}\boldsymbol{R}_0^2\right) \;\propto\; Z(\boldsymbol{R}_0) = e^{-\beta F(\mathsf{R}_0)}, \qquad (1)$$

where b is the monomer step length and N the number of steps of the chain trajectory. The entropic free energy of such a random walk, therefore, is given by the logarithm of the number of conformations with the fixed $\boldsymbol{R}_0$ and has the form $\beta F = -\ln P_0(\boldsymbol{R}_0) = \frac{3}{2Nb^2}\boldsymbol{R}_0^2 + \text{const}$, where $\beta = 1/k_B T$ the inverse Boltzmann temperature. At formation of the network, i.e. at crosslinking, each chain in the polymer melt obeys the distribution (1), which is then permanently frozen in the network topology.

One then assumes that the network junction points deform affinely with respect to their initial positions $\boldsymbol{R}_0$ following the macroscopic deformation described by the tensor $\underline{\underline{\lambda}}$; hence we can write $\boldsymbol{R} = \underline{\underline{\lambda}}\boldsymbol{R}_0$. Therefore, the deformation $\underline{\underline{\lambda}}$ alters the free energy of each strand. The change of entropic free energy per chain of the whole network can be calculated by the usual quenched averaging:

$$\beta F = -\langle \ln P(\boldsymbol{R})\rangle_{P(\mathsf{R}_0)} = \frac{1}{2}\mathrm{Tr}(\underline{\underline{\lambda}}^{\mathsf{T}}\underline{\underline{\lambda}}), \qquad (2)$$

where we have dropped an irrelevant constant, arising as the logarithm of the normalisation in (1). The overall elastic energy density, in the first approximation, is simply (2) multiplied by the number of elastically active network strands in the system n_{ch} per unit volume, which is proportional to the crosslinking density:

$$F_{\mathrm{elast}} = \frac{1}{2}\mu \,\mathrm{Tr}\left(\underline{\underline{\lambda}}^{\mathsf{T}}\underline{\underline{\lambda}}\right), \quad \text{with} \quad \mu = n_{\mathrm{ch}} k_B T. \tag{3}$$

Three positive remarks have to be made in defence of this simple model of rubber elasticity. First, consider the crosslinking connecting the end points of different polymer strands. Since the positions of end points of a single chain fluctuate strongly, the junctions reduce these fluctuations and therefore alter the single chain statistics. However, in spite of an apparent complexity, this effect merely introduces a multiplicative factor of the form $1-2/\phi$, where ϕ is the junction point functionality (see for example the review by Flory (1976)). Secondly, one can assume that the deformation preserves the volume, since the bulk (compression) modulus is by a factor of at least 10^4 greater than the shear modulus, which is proportional to μ; this implies the constraint $\det \underline{\underline{\lambda}} = 1$. Thirdly, the quenched average in equation (2) does not average over chains of different arc lengths, but the fact that the result is independent of arc length, generalises the result to apply for chains of arbitrary length, or even for a polydisperse ensemble of chains.

As a result if one considers, for example, a uniaxial extension λ (by incompressibility, the two perpendicular directions will experience an equal contraction $1/\sqrt{\lambda}$), the elastic energy would take the form $F_{\mathrm{elast}} = \frac{1}{2}\mu\,(\lambda^2 + 2/\lambda)$. This then allows us to calculate the nominal stress, which is the force divided by the area of the undeformed cross section:

$$\sigma_{\mathrm{phantom}} = \frac{\partial F}{\partial \lambda} = \mu\left(\lambda - \frac{1}{\lambda^2}\right) \tag{4}$$

Commonly, one draws the stress–strain curves in the Mooney-Rivlin representation, which plots the reduced stress function $f^* = \sigma/(\lambda - 1/\lambda^2)$ against $1/\lambda$ (see Fig. 2 in the discussion below). This representation therefore indicates the degree of deviation from the simple phantom chain network behaviour.

3 Reptation theory of rubber elasticity

Following the original ideas of Edwards (1977), we assume that each network strand is limited in its lateral fluctuations by the presence of neighbouring chains. Therefore each segment of a polymer only explores configurations in

a limited volume, which is much smaller than the space occupied by an ideal random coil. Hence, the whole strand fluctuates around a certain trajectory, a mean path, which is called the primitive path in the reptation theory (Edwards 1977). The most intuitive way to visualise such a trajectory is to imagine that the chain is made shorter and thus stretched between the fixed crosslinking points. The taut portions of the chain will form the broken line of straight segments between the points of entanglement, which restrict the further tightening. This primitive path can be considered as a random walk with an associated typical step length, which is much bigger than the polymer step length, as sketched in Fig. 1. The number of corresponding tube segments M is determined by the average number of entanglements per chain (the situation with no entanglements corresponds to $M = 1$).

Effectively, the real polymer is confined by the neighbouring chains to exercise its thermal motion only within a tube around the primitive path. Note that all the chains are in constant thermal motion, altering the local constraints they impose on each other. Hence, the fixed tube is a gross simplification of the real situation. However, one expects this to be an even better approximation in rubber than in a corresponding melt (where the success of reptation theory is undeniable), because the restriction on chain reptation diffusion in a crosslinked network eliminates the possibility of constraint release.

To handle the tube constraint mathematically, we traditionally assume that the chain segments are subjected to a quadratic potential, restricting their motion transversely to the primitive path. Along one polymer strand consisting of N monomers of effective step length b, there are M tube segments, each containing s_m, $m = 1, \ldots, M$ monomer steps. We infer the obvious condition

$$\sum_{m=1}^{M} s_m = N. \tag{5}$$

In effect, one has two random walks: the topologically fixed primitive path and the polymer chain restricted to move around it – both having the same end-to-end vector $\boldsymbol{R}_0$, between the connected crosslinking points.

Each tube segment m can be described by the span vector $\boldsymbol{\Delta}_m$, joining the equilibrium positions of the strand monomers at the two ends of each tube segments. The number of tube segments M (or, equivalently, the nodes of the primitive path) is a free parameter of the theory, ultimately determined by the length of each polymer strand and the entanglement density.

Since the primitive path is a topologically frozen characteristic of each network strand, we shall assume that all primitive path spans $\boldsymbol{\Delta}_m$ deform affinely with the macroscopic strain: $\boldsymbol{\Delta}'_m = \underline{\underline{\lambda}}\boldsymbol{\Delta}_m$. This is the central point

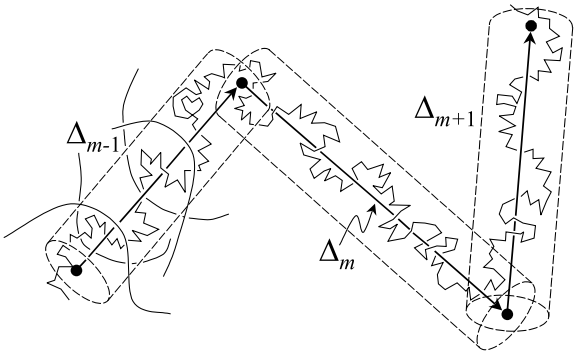

Figure 1: A polymer strand is surrounded by neighbouring chains, which effectively confine the strand to a tube. The tube segment m, with the span vector $\mathbf{\Delta}_m$ along its axis, contains s_m monomer steps, where m runs from 1 to M.

in the model: the rubber elastic response will arise due to the change in the number of polymer configurations in a distorted primitive path. To evaluate the number of conformations, we look separately at chain excursions parallel and perpendicular to the tube axis, along each span $\mathbf{\Delta}_m$. Effectively, this amounts to introducing a new coordinate system for each tube segment, with one preferred axis along $\mathbf{\Delta}_m$. In this direction one recovers the behaviour of a free random walk, giving rise to a one-dimensional Gaussian statistics in the long chain limit. Note that only one third of the steps s_m in this tube segment would be involved in such parallel (longitudinal) excursions. We therefore obtain for the number of parallel excursions in a tube segment m:

$$W_m^{\parallel} \propto \frac{1}{\sqrt{s_m/3}} \exp\left(-\frac{1}{2b^2(s_m/3)}\mathbf{\Delta}_m^2\right). \tag{6}$$

To determine the number of perpendicular (transverse) excursions, one can introduce the Green's function for the perpendicular steps made by the chain. In effect, we consider a two-dimensional random walk, with a total number of steps $(2s_m/3)$, in a centrosymmetric quadratic potential. For each of these two perpendicular coordinates, the Green's function satisfies the following modified diffusion equation (see e.g. Doi & Edwards 1986):

$$\left(\frac{\partial}{\partial s} - \frac{b^2}{2}\frac{\partial^2}{\partial x_f^2} + \frac{q_0^2}{2}x_f^2\right) G(x_i, x_f; s) = \delta(x_f - x_i)\delta(s), \tag{7}$$

where the x_i and x_f are the initial and final coordinates of the random walk with respect to the tube axis and q_0 determines the strength of the

confining potential. This is an essential parameter of many reptation theories, directly related to the tube diameter a. Many discussions can be found in the literature regarding, for instance, the possible dependence of a on entanglement density and the possible change in a on deformation. However, we shall find that the potential strength q_0 does not enter the final rubber-elastic energy, in an approximation that we expect to hold for a majority of cases. Such a universality resembles the situation with phantom networks, where many chain parameters do not contribute to the final results.

The equation (7) is very common in the physics of polymers and its exact solution is known. However, we only need to consider a particular limit $q_0 b s_m \gg 1$ of this solution, which is the case of dense entanglements (resulting in a strong confining potential) and/or of a large number s_m of monomers confined in the tube segment. Outside this limit, that is, when the tube diameter is the same order as the arc length of the confined chain, the whole concept of chain entanglements becomes irrelevant. In the case of our present interest, that is, in the strongly confined limit, the solution has a particularly simple form, see (Edwards (1977),

$$G_m(x_i, x_f; s_m) \propto \exp\left(-\frac{q_0}{2b}(x_i^2 + x_f^2) - \frac{1}{6} q_0 b s_m\right). \tag{8}$$

Remembering that there are two coordinates describing the transverse excursions, we obtain for the two-dimensional Green's function of the tube segment m:

$$G_m(\boldsymbol{r}_i, \boldsymbol{r}_f; s_m) \propto \exp\left(-\frac{1}{3} q_0 b s_m\right) \exp\left(-\frac{q_0}{2b}(\boldsymbol{r}_i^2 + \boldsymbol{r}_f^2)\right), \tag{9}$$

where $\boldsymbol{r}_i$ and $\boldsymbol{r}_f$ are the initial and final transverse two-dimensional coordinates.

The total number of transverse excursions is proportional to the integrated Green's function:

$$W_m^{\perp} \propto \int d\boldsymbol{r}_i \int d\boldsymbol{r}_f G_m(\boldsymbol{r}_i, \boldsymbol{r}_f; s_m).$$

Since the Green's function in the approximation (9) does not couple the initial or final coordinates to the number of segments s_m, this integration will only produce a constant normalisation factor which can be discarded.

Gathering the expressions for statistical weights of parallel and perpendicular excursions, we obtain the total number of configurations of a polymer segment consisting of s_m monomers in a tube segment of span $\boldsymbol{\Delta}_m$:

$$W_m = W_m^{\parallel} W_m^{\perp} \propto \frac{1}{\sqrt{s_m}} \exp\left(-\frac{3}{2b^2 s_m} \boldsymbol{\Delta}_m^2 - \frac{1}{3} q_0 b s_m\right). \tag{10}$$

Therefore, we find for the full number of configurations of the whole strand by summing over all M steps of the primitive path and integrating over the remaining degrees of freedom, the number of polymer segments confined between each node of the tube:

$$W = \int_0^N ds_1 \cdots \int_0^N ds_M \left(\prod_{m=1}^{M} W_m \right) \delta \left(\sum_{m=1}^{M} s_m - N \right), \tag{11}$$

where the constraint (5) on the polymer contour length is implemented by the delta-function. The statistical summation in (11) takes into account the reptation motion of the polymer between its two crosslinked ends, by which the number of segments, s_m, constrained within each tube segment can be changed and, thus, equilibrates for a given conformation of primitive path.

Rewriting the delta-function as $\delta(x) = \frac{1}{2\pi} \int dk \; e^{\mathrm{i}kx}$, we proceed by finding the saddle points s_m^* which make the exponent of the statistical sum (11) stationary. It can be verified that the normalisation factors $1/\sqrt{s_m}$ contribute only as a small correction to the saddle points

$$s_m^* \approx \left(\frac{3\boldsymbol{\Delta}_m^2}{2b^2(\frac{1}{3}q_0 b + \mathrm{i}k)} \right)^{1/2}. \tag{12}$$

The integral in (11) is consequently approximated by the steepest descent method. We repeat the same procedure for the integration of the auxiliary variable k, responsible for the conservation of the polymer arc length. The saddle point value k^*, inserted back into (12), gives the equilibrium number of polymer segments confined within a tube segment with the span vector $\boldsymbol{\Delta}_m$:

$$\overline{s_m} = \frac{N\Delta_m}{\sum_{m=1}^{M} \Delta_m}, \tag{13}$$

where $\Delta_m = |\boldsymbol{\Delta}_m|$ is the length of the m-th step of the primitive path. We finally obtain the total number of configurations of one strand, confined within a tube whose primitive path is described by the set of vectors $\{\boldsymbol{\Delta}_m\}$. The statistical weight W associated with this state is proportional to the probability distribution:

$$W(\boldsymbol{\Delta}_1, \ldots, \boldsymbol{\Delta}_M) \propto P(\{\boldsymbol{\Delta}_m\}) \propto e^{-\frac{1}{3}q_0 bN} \frac{\exp\left(-\frac{3}{2b^2 N} \left(\sum_{m=1}^{M} \Delta_m \right)^2 \right)}{\left(\sum_{m=1}^{M} \Delta_m \right)^{M-1}}. \tag{14}$$

This expression is a result corresponding to the ideal Gaussian $P_0(\boldsymbol{R}_0)$ in equation (1) for a non-entangled phantom chain. Note that the chain end-to-end distance $\boldsymbol{R}_0$ is also the end-to-end distance of the primitive path random

walk of variable-length steps: $\sum_{m=1}^{M} \boldsymbol{\Delta}_m = \boldsymbol{R}_0$. The probability distribution $P(\{\boldsymbol{\Delta}_m\})$ for a chain confined in a reptation tube is reminiscent of a normal Gaussian, but is in fact significantly different in the form of the exponent and the denominator (note the modulus of the tube segment vector $\boldsymbol{\Delta}_m$).

From equation (14) we obtain the formal expression for free energy of a chain confined to a tube with the primitive path conformation $\{\boldsymbol{\Delta}_m\}$, which implicitly depends on the end-to-end vector $\boldsymbol{R}_0$ (the separation between crosslink points):

$$\beta F = \frac{3}{2b^2 N} \left(\sum_{m=1}^{M} \Delta_m \right)^2 + (M-1) \ln \left(\sum_{m=1}^{M} \Delta_m \right), \tag{15}$$

4 Free energy of deformations

We now perform a procedure which is analogous to the one used to obtain equation (2). In the polymer melt before crosslinking, the ensemble of chains obeys the distribution in (14) giving the free energy per strand (15). The process of crosslinking not only quenches the end points of each of the crosslinked strands, but also quenches the nodes of the primitive path $\boldsymbol{\Delta}_m$, since the crosslinked chains cannot disentangle due to the fixed network topology. In our mean field approach, the tube segments described by $\boldsymbol{\Delta}_m$ are conserved, although they may be deformed by the strains applied to the network. For evaluating the quenched average, note that the statistical weight (14) treats the tube segments m in a symmetric way. This allows us to perform the explicit summation over the index m:

$$\begin{aligned} \beta F &= \left\langle \frac{3}{2b^2 N} \left(\sum_{m=1}^{M} \Delta_m \right)^2 + (M-1) \ln \left(\sum_{m=1}^{M} \Delta_m \right) \right\rangle \\ &= \frac{3}{2b^2 N} \left(M \left\langle \Delta_m^2 \right\rangle + M(M-1) \left\langle \Delta_m \Delta_n \right\rangle \right) \\ &\quad + (M-1) \left\langle \ln \left(\sum_{m=1}^{M} \Delta_m \right) \right\rangle, \end{aligned} \tag{16}$$

where, in the second term, m and $n \neq m$ are arbitrary indices of the primitive path steps. The brackets $\langle \cdots \rangle$ refer to the average with respect to the weight $P(\{\boldsymbol{\Delta}_m\})$ given in (14).

Furthermore, note that any affine deformation $\underline{\underline{\lambda}}$ transforms the vectors $\boldsymbol{\Delta}_m$ into $\boldsymbol{\Delta}_m' = \underline{\underline{\lambda}} \boldsymbol{\Delta}_m$ and, hence, their lengths $\Delta_m = |\boldsymbol{\Delta}_m|$ into $\Delta_m' = |\underline{\underline{\lambda}} \boldsymbol{\Delta}_m|$, but leaves the quenched distribution $P(\{\boldsymbol{\Delta}_m\})$ unchanged. Bearing this in mind, we can evaluate the averages (16), leading to the free energy per chain

of the crosslinked network. The Appendix gives a more detailed account of how one evaluates the averages. The resulting average elastic energy density also incorporates the density of crosslinked chains in the system by the constant $\mu = n_{\rm ch} k_B T$:

$$\begin{aligned} F_{\rm elast} &= \frac{2}{3}\mu \frac{2M+1}{3M+1} {\rm Tr}(\underline{\underline{\lambda}}^{\mathsf{T}} \underline{\underline{\lambda}}) \\ &+ \frac{3}{2}\mu\,(M-1)\frac{2M+1}{3M+1}(\overline{|\underline{\underline{\lambda}}|})^2 + \mu(M-1)\overline{\ln|\underline{\underline{\lambda}}|}, \end{aligned} \tag{17}$$

where the following notations are employed:

$$\overline{|\underline{\underline{\lambda}}|} = \frac{1}{4\pi}\int_{|\boldsymbol{e}|=1} d\Omega\ |\underline{\underline{\lambda}}\ \boldsymbol{e}| \tag{18}$$

$$\overline{\ln|\underline{\underline{\lambda}}|} = \frac{1}{4\pi}\int_{|\boldsymbol{e}|=1} d\Omega\ \ln|\underline{\underline{\lambda}}\ \boldsymbol{e}|. \tag{19}$$

The notation $\overline{\cdots}$ refers to the angular integration over a unit vector $\boldsymbol{e}$.

In the case of uniaxial deformation, where $\underline{\underline{\lambda}}$ takes a diagonal form with $\lambda^{\parallel} = \lambda$ and $\lambda^{\perp} = 1/\sqrt{\lambda}$, the expressions (18) and(19) can be calculated explicitly. The Appendix contains the formulae (equations (22) - (24)), which need to be inserted into (17) to give the full rubber-elastic energy density. In the small deformation limit, where $\lambda = 1 + \varepsilon$, expression (17) immediately leads to the Young's modulus E in $F_{\rm ext} \approx \frac{1}{2}E\varepsilon^2$ after noting that

$$\begin{aligned} {\rm Tr}(\underline{\underline{\lambda}}^{\mathsf{T}} \underline{\underline{\lambda}}) &\approx 3 + 3\ \varepsilon^2 \\ \overline{|\underline{\underline{\lambda}}|} &\approx 1 + \frac{2}{5}\varepsilon^2 \\ \overline{\ln|\underline{\underline{\lambda}}|} &\approx \frac{3}{10}\varepsilon^2. \end{aligned}$$

For small simple shear, we can write the matrix $\underline{\underline{\lambda}}$ as $\lambda_{ij} = \delta_{ij} + \varepsilon u_i v_j$, where $\boldsymbol{u}$ and $\boldsymbol{v}$ are two orthogonal unit vectors. As expected, the shear modulus G in $F_{\rm shear} \approx \frac{1}{2}G\varepsilon^2$ is one third of the Young's modulus E:

$$G = \frac{1}{3}E = \mu\left(\frac{4}{3}\cdot\frac{2M+1}{3M+1} + \frac{1}{5}(M-1)\cdot\frac{11M+5}{3M+1}\right). \tag{20}$$

We point out that the expression (17) is nearly identical to the rubber elastic free energy density obtained by Higgs and Ball (1989), although they start from a completely different set of physical and assumptions and mathematical framework. In HB, the entanglements make the strands to interact with each other only at certain points. This is modelled by forcing

the individual strands to pass through a certain number of hoops. They effectively divide the polymer strand into segments, each performing a three-dimensional phantom random walk. In this approach, the entanglements only exert constraints at points and allow the polymer to obey free Gaussian statistics between these interaction points. Nevertheless, the apparent identity of the final expression for the rubber-elastic free energy density is a comforting reflection of consistency in underlying physical concepts and the mathematical treatment of both models. The internal similarity of the models arises from the treatment of local chain reptation, equilibrating the distribution of its segments between the nodes of primitive path, before and after the deformation.

From the expression (17), we can recover the ordinary free energy of a phantom chain network by taking the case $M = 1$: $F_{\rm elast} = \frac{1}{2}\mu {\rm Tr}(\underline{\underline{\lambda}}^{\mathsf{T}}\underline{\underline{\lambda}})$. This limit means physically that the polymer strand is placed in one single tube, tightly confined to the axis. Mathematically, a random walk in three dimensions with the total of N steps is equivalent to a random walk in one dimension along a given direction $\mathbf{\Delta}$, with $N/3$ steps, while the two perpendicular excursions in a tightly confining potential do not contribute to the global elastic response. This fact is the underlying reason why we recover the phantom chain network result by taking $M = 1$ in our model. Of course, in a parallel "hoop model" of HB the case $M = 1$ simply means that there are no constraints.

On the other hand, as the number of tube segments M becomes very large, we obtain a rubber-elastic elastic energy of the form

$$F_{\rm elast} = \mu\, M\Big((\overline{|\underline{\underline{\lambda}}|})^2 + \overline{\ln |\underline{\underline{\lambda}}|}\Big). \tag{21}$$

There are two ways to arrive at this limit of $M \gg 1$ in a real physical situation: either the polymer melt is very dense, causing a high entanglement density, or the polymer chain is very long. In the latter case, the polymer strand experiences many confining entanglements along its path.

Recall that the $F_{\rm elast}$ is the elastic energy density, which relates to the free energy per chain, such as the eq. (15), and is proportional to the density of elastic strands in the system: $F_{\rm elast} \propto \mu = n_{\rm ch} k_B T$, where $n_{\rm ch}$ is the number of crosslinked strands per unit volume. We can assume that in a melt, or a semidilute solution, the chain density is inversely proportional to the volume of an average chain, hence inversely proportional to the chain contour length: $n_{\rm ch} \propto 1/L$. In the case of phantom network with a free energy $F_{\rm elast} = \frac{1}{2}\mu {\rm Tr}(\underline{\underline{\lambda}}^{\mathsf{T}}\underline{\underline{\lambda}})$, one conclude that $F_{\rm elast} \to 0$ as the chains become infinitely long! This unphysical result reflects the fact that the phantom chain model assumes the entanglement interactions of the chains irrelevant.

Clearly, this assumptions breaks down in the long chain limit, where we expect the entanglements to play a crucial role.

This unphysical feature of phantom network model is overcome by our expression (21). As the strands become longer, they will experience more entanglements, generating more primitive path nodes and confining tube segments. One can assume that the number of entanglements scales linearly with the strand length L: $M \propto L$, in fact: $M = N/N_e$ with N_e the characteristic entanglement length, essentially the average of s_m^*. Considering expression (21), with $n_{\mathrm{ch}} = 1/v_{\mathrm{monomer}}N$ (the inverse volume of the chain in a melt), we note that the corresponding elastic free energy F_{elast} does not vanish in the limit $L \to \infty$. At $M \gg 1$ the constant plateau modulus becomes $\mu M = k_B T/v_{\mathrm{monomer}}N_e$. As one expects, in an entangled polymer system there is no real difference between the network and the melt and they both have the same plateau modulus – with the corollary that the entanglement length N_e must be much smaller in the permanently crosslinked network.

5 Conclusion

In this present work, we have analysed the behaviour of a polymer network in presence of entanglements, which are treated within a classical mean-field tube model. We found that this leads to an elastic energy which is identical to the one derived in the hoop model of HB (Higgs & Ball 1989). We claim that our model captures the physics of entanglements in a better way than HB, since the entanglements at a microscopic level do not so much localise the polymer at fixed points in space along its path, but rather impede the chain fluctuations on a length scale which is much larger than the size of monomers. This is due to the fact that the entanglements are caused by neighbouring strands, which likewise fluctuate. In this sense, our model provides a firmer ground of the theoretically known and experimentally tested results.

Since our results for the isotropic rubber are identical to the ones by HB and theirs have been extensively compared with experimental data in a review by Higgs & Gaylord (1990), we do not need to include a similar comparison here. We only remark that the theoretically predicted curve for the reduced stress function f^* agrees with the experimental data to a good level, see Fig. 2.

Our model only describes the equilibrium response of a network to deformation. Shortly after applying the deformation, traditionally assumed affine on the level of primitive path segments, the network finds its chains far from the microscopic equilibrium. Each strand then redistributes its monomers between the deformed the tube segments, attributing more monomers to

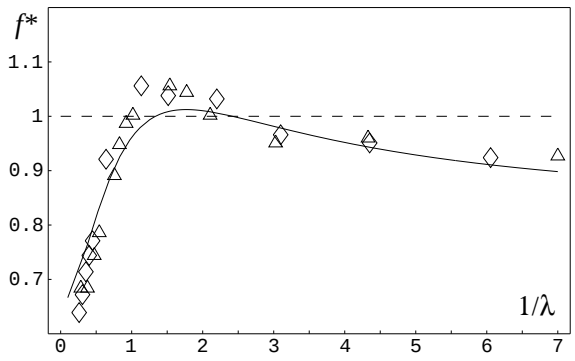

Figure 2: The Mooney-Rivlin plot: the reduced stress function $f^* = \sigma/(\lambda - 1/\lambda^2)$ plotted against $1/\lambda$. Data points from the analysis of ref. (Gaylord & Douglas 1990) are fitted by the result arising from full rubber-elastic energy (17). Fitting indicates that $M \gg 1$ and the equation (21) is a good approximation.

some segments, less to others. This process proceeds via the local reptation, the sliding motion along the primitive path, and would be reflected by a time dependence of the variable s_m. This number of monomers attributed to the tube segment m is changing, after the deformation, between a the initial value s_m^* in the Eq. (13) and the corresponding saddle-point value at $\Delta'_m = |\underline{\underline{\lambda}}\boldsymbol{\Delta}_m|$. By describing the associated relaxation process, our model can be naturally extended to describe the short-time viscoelastic response of an ideal crosslinked network (with no loops and dangling ends, leading to long relaxation of stress); the characteristic time of such a reptation dynamics is the Rouse time, since the dominant process is the monomer diffusion along the principal path.

We appreciate many valuable discussions with S. F. Edwards. S. K. gratefully acknowledges support from an Overseas Research Scholarship, from the Cambridge Overseas Trust and from Corpus Christi College.

Evaluation of quenched averages $\langle \Delta_m \Delta_n \rangle$ and $\langle \ln(\sum \Delta_m) \rangle$

To evaluate the thermodynamic average $\langle \Delta_m \Delta_n \rangle$, $m, n = 1, \ldots, N$ in the general case, one needs to average $\Delta_m \Delta_n = |\boldsymbol{\Delta}_m||\boldsymbol{\Delta}_n|$ with the probability distribution given by Eq. (14). For this purpose, one first has to find the normalisation $\hat{\mathcal{N}}$ of the distribution, which can most easily be achieved by

introducing a new scalar variable $u = \sum_{m=1}^{M} \Delta_m$ to simplify the exponent of this distribution:

$$\begin{aligned}
\hat{\mathcal{N}} &= \prod_{m=1}^{M} \int d\mathbf{\Delta}_m \frac{\exp\left(-\frac{3}{2b^2N}\left(\sum_{m=1}^{M}\Delta_m\right)^2\right)}{\left(\sum \Delta_m\right)^{M-1}} \\
&= \prod_{m=1}^{M} \int d\mathbf{\Delta}_m \int_0^\infty du\ \delta\left(u - \sum_{m=1}^{M}\Delta_m\right) \frac{e^{-\frac{3}{2b^2N}u^2}}{u^{M-1}} \\
&= (4\pi)^M \int_0^\infty du \frac{e^{-\frac{3}{2b^2N}u^2}}{u^{M-1}} \underline{\int_0^u d\Delta_1 \Delta_1^2 \int_0^{u-\Delta_1} d\Delta_2 \Delta_2^2 \cdots} \\
&\qquad \underline{\int_0^{u-\ldots-\Delta_{M-2}} d\Delta_{M-1}\Delta_{M-1}^2 \cdot (u - \Delta_1 - \ldots - \Delta_{M-1})^2}
\end{aligned}$$

In the last step, we introduced spherical coordinates for the variables $\mathbf{\Delta}_m$, implemented the constraint $u = \sum \Delta_m$ and used the fact that the variables Δ_m are bound to be positive. The underlined expression is a function of u, which we call $I_M(u)$. Since the integrals only involve power functions, $I_M(u)$ itself is a power in u, whose order can be determined by counting the dimensions:

$$I_M(u) = \frac{1}{X_M} u^{3M-1}.$$

After noting the recursive structure of $I_M(u)$, one can find a recursion relation for the coefficients X_M:

$$X_{M+1} = \frac{1}{2} 3M(3M+1)(3M+2) X_M.$$

Since $I_{M=1}(u) = u^2$, all coefficients X_M and hence all functions $I_M(u)$ are known. The remaining integration of u is a standard Gaussian integral.

Having obtained the normalisation constant $\hat{\mathcal{N}}$, we can proceed to calculate the averages $\langle \Delta_m \Delta_n \rangle$. The calculations are very similar to the above one for $\hat{\mathcal{N}}$; the only significant difference is the angular part of the integration which produces terms of the form $\frac{1}{3}\mathrm{Tr}(\underline{\underline{\lambda}}^{\mathsf{T}}\underline{\underline{\lambda}})$ and $\overline{|\underline{\underline{\lambda}}|}$ for the case $m = n$ or $m \neq n$ respectively.

For the logarithmic term, one in fact finds that only the angular integration yields relevant terms:

$$\left\langle \ln\left(\sum_{m=1}^{M}\Delta_m\right)\right\rangle =$$

$$\frac{1}{\hat{\mathcal{N}}}\int_0^\infty du\frac{e^{-\frac{3}{2b^2N}u^2}}{u^{M-1}}\int_0^u d\Delta_1\Delta_1^2\int_0^{u-\Delta_1}d\Delta_2\Delta_2^2\cdots$$
$$\int_0^{u-\ldots-\Delta_{M-2}}d\Delta_{M-1}\Delta_{M-1}^2\,(u-\Delta_1-\ldots-\Delta_{M-1})^2$$
$$\left(\prod_{m=1}^{M}\int d\Omega_m\right)\ln[\Delta_1|\underline{\underline{\lambda}}\boldsymbol{e}_1|+\ldots+\Delta_{M-1}|\underline{\underline{\lambda}}\boldsymbol{e}_{M-1}|$$
$$+(u-\Delta_1-\ldots-\Delta_{M-1})|\underline{\underline{\lambda}}\boldsymbol{e}_M|]$$

with the unit vector $\boldsymbol{e}_m$ specifies the (arbitrary) orientation of the corresponding tube segment $\boldsymbol{\Delta}_m$. Then one observes:

$$\begin{aligned}
&\ln\left[\Delta_1|\underline{\underline{\lambda}}\boldsymbol{e}_1|+\ldots+\Delta_{M-1}|\underline{\underline{\lambda}}\boldsymbol{e}_{M-1}|+(u-\Delta_1-\ldots-\Delta_{M-1})|\underline{\underline{\lambda}}\boldsymbol{e}_M|\right]\\
&= \ln[u]+\ln[|\underline{\underline{\lambda}}\boldsymbol{e}_M|]+\ln\left[1+\underbrace{\sum_{m=1}^{M-1}\left(\frac{|\underline{\underline{\lambda}}\boldsymbol{e}_m|}{|\underline{\underline{\lambda}}\boldsymbol{e}_M|}-1\right)\frac{\Delta_m}{u}}_{\text{small since } u\gg|\boldsymbol{\Delta}_m|}\right]\\
&\approx \ln[|\underline{\underline{\lambda}}\boldsymbol{e}_M|]+\text{const.}
\end{aligned}$$

In case of uniaxial deformation, the evaluation of $\mathrm{Tr}(\underline{\underline{\lambda}}^{\mathsf{T}}\underline{\underline{\lambda}})$, $\overline{|\underline{\underline{\lambda}}|}$ and $\overline{\ln|\underline{\underline{\lambda}}|}$, cf. equations (17) – (19) has been given elsewhere (Higgs & Gaylord 1990), but for completeness we state them here as well:

$$\mathrm{Tr}(\underline{\underline{\lambda}}^{\mathsf{T}}\underline{\underline{\lambda}}) = \lambda^2+\frac{1}{\lambda} \tag{22}$$

$$\overline{|\underline{\underline{\lambda}}|} = \frac{1}{2}\left(\lambda+\frac{1}{2\sqrt{\lambda}\sqrt{\lambda^3-1}}\ln\left(\frac{\lambda^{3/2}+\sqrt{\lambda^3-1}}{\lambda^{3/2}-\sqrt{\lambda^3-1}}\right)\right) \tag{23}$$

$$\overline{\ln(|\underline{\underline{\lambda}}|)} = \ln(\lambda)-1+\frac{\arctan\sqrt{\lambda^3-1}}{\sqrt{\lambda^3-1}}, \tag{24}$$

References

[1] Abramchuk, S. S., Nyrkova, I. A. & Khokhlov, A. R. 1989 An elasticity theory of rubbers with orientational interactions. *Polymer Science U.S.S.R.* **31**, 1936–1945.

[2] Ball, R. C., Doi, M., Edwards, S. F. & Warner, M. 1981 Elasticity of entangled networks *Polymer* **22**, 1010–1018.

[3] Bladon, P. & Warner, M. 1993 Elasticity of nematic networks and nematic effects in conventional rubbers. *Macromolecules* **26**, 1078–1085.

[4] Deloche, B. & Samulski, E. T. 1981 Short-range nematic-like orientational order in strained elastomers - a deuterium magnetic-resonance study. *Macromolecules* **14**, 575–581.

[5] Doi, M. & Edwards, S. F. 1986 *Theory of Polymer Dynamics.* Oxford: Clarendon Press.

[6] Doi, M., Pearson, D., Kornfield, J., & Fuller, G. 1989 Effect of nematic interaction in the orientational relaxation of polymer melts. *Macromolecules* **22**, 1488–1490.

[7] Edwards, S. F. 1977 The theory of rubber elasticity. *Brit. Polymer J.* June 1977, 140–143.

[8] Edwards, S. F. & Vilgis T. A. 1988 The tube model - Theory of rubber elasticity. *Rep. Prog. Phys.* **51**, 243-297.

[9] Flory, P. J. 1976 Statistical thermodynamics of random networks. *Proc. R. Soc. Lond. A.* **351**, 351-380.

[10] Flory, P. J. & Erman, B. 1982 Theory of elasticity of polymer networks. *Macromolecules* **15**, 800–806 (1982).

[11] Gaylord, R. J. & Douglas, J. F. 1990 The localization model of rubber elasticity. *Polymer Bulletin* **23**, 529–533.

[12] Gennes, de, P. G. 1979 *Scaling Concepts in Polymer Physics.* Ithaca (N.Y.): Cornell University Press.

[13] Han, W. H., Horkay, F., & McKenna, G. B. 1999 Mechanical and swelling behaviors of rubber: A comparison of some molecular models with experiment. *Mathematics and Mechanics of Solids* **4**, 139–167.

[14] Heinrich, G., Helmis, G. & Vilgis, T. 1995 Polymer networks - state-of-art of the molecular-statistical theory. *Kautschuk, Gummi, Kunststoffe* **10**, 689.

[15] Higgs, P. G. & Ball, R. C. 1989 Trapped entanglements in rubbers - a unification of models. *Europhys. Lett.* **8**, 357–361.

[16] Higgs, P. G. & Gaylord, R. J. 1990 Slip-links, hoops and tubes - tests of entanglement models of rubber elasticity. *Polymer* **31**, 70–74.

[17] Jarry, J.-P. & Monnerie, L. 1979 *Macromolecules* **12**, 316 (1979).

This figure "fig1.jpg" is available in "jpg" format from:

http://ttt.lanl.gov/ps/cond-mat/0106371

This figure "fig2.jpg" is available in "jpg" format from:

http://ttt.lanl.gov/ps/cond-mat/0106371